Human Molecular Genetics, 2017, Vol. 26, No. 19 3823–3836

doi: 10.1093/hmg/ddx269
Advance Access Publication Date: 11 July 2017
Original Article

ORIGINAL ARTICLE

NCEH-1 modulates cholesterol metabolism and protects against α-synuclein toxicity in a *C. elegans* model of Parkinson's disease

Siyuan Zhang[1], Samantha A. Glukhova[1], Kim A. Caldwell[1,2] and Guy A. Caldwell[1,2,*]

[1]Department of Biological Sciences, The University of Alabama, Tuscaloosa, AL 35487, USA and [2]Departments of Neurology and Neurobiology, Center for Neurodegeneration and Experimental Therapeutics, The University of Alabama School of Medicine at Birmingham, Birmingham, AL 35294, USA

*To whom correspondence should be addressed. Tel: 205 3489926; Fax: 205 3481786; Email: gcaldwel@ua.edu

Abstract

Parkinson's disease (PD) is an aging-associated neurodegenerative disease affecting millions worldwide. Misfolding, oligomerization and accumulation of the human α-synuclein protein is a key pathological hallmark of PD and is associated with the progressive loss of dopaminergic neurons over the course of aging. Lifespan extension via the suppression of IGF-1/insulin-like signaling (IIS) offers a possibility to retard disease onset through induction of metabolic changes that provide neuroprotection. The *nceh-1* gene of *Caenorhabditis elegans* encodes an ortholog of neutral cholesterol ester hydrolase 1 (NCEH-1), an IIS downstream protein that was identified in a screen as a modulator of α-synuclein accumulation *in vivo*. The mechanism whereby cholesterol metabolism functionally impacts neurodegeneration induced by α-synuclein is undefined. Here we report that NCEH-1 protects dopaminergic neurons from α-synuclein-dependent neurotoxicity in *C. elegans* via a mechanism that is independent of lifespan extension. We discovered that the presence of cholesterol, LDLR-mediated cholesterol endocytosis, and cholesterol efflux are all essential to NCEH-1-mediated neuroprotection. In protecting from α-synuclein neurotoxicity, NCEH-1 also stimulates cholesterol-derived neurosteroid formation and lowers cellular reactive oxygen species in mitochondria. Collectively, this study augments our understanding of how cholesterol metabolism can modulate a neuroprotective mechanism that attenuates α-synuclein neurotoxicity, thereby pointing toward regulation of neuronal cholesterol turnover as a potential therapeutic avenue for PD.

Introduction

Parkinson's Disease (PD) is the second most common neurodegenerative disorder, characterized by progressive dopaminergic (DA) neuron death in the *pars compacta* region of the *substantia nigra* and the accumulation of insoluble α-synuclein (α-syn) forming Lewy bodies. Cholesterol has an important role in CNS synaptogenesis and is necessary for optimal neurotransmitter release (1). The impact of cholesterol on neurodegeneration has been debated and is an unresolved area of investigation. Whereas some studies show that low levels of plasma cholesterol correlate with the occurrence of PD (2–4), another study provided contradictory findings (5). In rodent models of PD, high fat diet exacerbated the 1-methyl-4-phenyl-, 2, 3, 6-tetrahydropyridine (MPTP)-induced depletion of striatal dopamine (6). Hydroxylated cholesterol metabolites were reported as significantly high in PD patients (7,8). Furthermore, lipid homeostasis has been proposed to influence the localization, fibrilization and neurotoxicity of α-syn (9–11). Nevertheless, the mechanism

Received: May 11, 2017. **Revised:** June 29, 2017. **Accepted:** July 6, 2017

by which cholesterol metabolism modulates PD pathology remains elusive.

The Insulin-like Signaling (IlS) pathway is implicated in aging and neurodegeneration (12). In *C. elegans*, mutation in the gene encoding DAF-2, the sole insulin-like receptor in this nematode, is well-known for its extension of lifespan (13). In a previously reported RNAi screen designed to reveal functional modulators at the intersection of aging and PD using transgenic worms overexpressing human α-syn in combination with *daf-2* mutation, we identified NCEH-1 (neutral cholesterol ester hydrolase-1) as a gene product whose knockdown enhanced α-syn misfolding in the body wall muscle cells of *C. elegans* (14). Notably, the transcription of *C. elegans nceh-1* is positively regulated by a block of IIS (15); insulin deficiency also up-regulates cholesterol synthesis in the brain (16).

Human neutral cholesterol ester hydrolase (NCEH) protein is reported to be highly expressed in brain (cerebral cortex, hippocampus and caudate), lung and gastrointestinal tract; medium-level expression is detected in endocrine tissues, bone marrow, the immune system and muscle tissues; NCEH can be also detected in tissues such as liver, gallbladder, pancreas, kidney, urinary bladder, adipose tissue, skin and reproductive organs with a low expression rate [www.proteinatlas.org;(17)]. Similarly, *C. elegans nceh-1* exhibits expression at all stages of development and in adults (18). Additionally, *nceh-1* is likely to be expressed ubiquitously in worms, as RNAi knockdown results in phenotypic changes in multiple tissues including DA neurons, body-wall muscles, and intestine (14; this study).

In mammals, NCEH is a single-membrane-spanning type II membrane protein comprised of three domains: N-terminal, catalytic, and lipid-binding. The N-terminal domain serves as a type II signal anchor sequence to recruit NCEH to the endoplasmic reticulum (ER), with its catalytic domain positioned within the lumen (19). NCEH activity has been previously implicated in a variety of disease states. For example, NCEH was found to be associated with macrophages in atherosclerotic lesions where it contributes to the initial step of reverse cholesterol transport (20). This enzyme was also reported to be highly elevated in aggressive cancer cells, serving as a central node in an ether lipid signaling network that bridges platelet-activating factor and lysophosphatidic acid (21). Interestingly, the transcription of NCEH is also down-regulated in skin fibroblasts from Alzheimer's disease patients (22).

It is important to note that *C. elegans* is a cholesterol auxotroph, whereby cholesterol, obtained exogenously, is primarily used as a precursor of reproductive signaling (23). Although mammals are capable of biosynthesizing cholesterol, the blood brain barrier partitions the passage of peripheral cholesterol. In the adult state, mammalian neurons rely on delivery of cholesterol from nearby astrocytes, thereby facilitating local resource allocation toward the generation of electrical impulse and dispensing with the energetic cost for cholesterol synthesis (24). *C. elegans* DA neurons are also anatomically adjacent to, and are sheathed by glia that may represent an analogous cholesterol reservoir (25). Importantly, *C. elegans* possesses a remarkable advantage in studying cholesterol metabolism in the context of neurodegeneration, whereby the lack of *de novo* cholesterol biosynthesis represents a means for the receipt of cholesterol that is more comparable to the situation in adult mammalian neurons in the brain. This makes the function of NCEH-1 prominent by liberating metabolically active free cholesterol from intracellularly-stored cholesterol esters. In this report, NCEH-1, a modulator of cholesterol metabolism, is evaluated for the first time as a functional modifier of α-syn-induced neurotoxicity.

Results

Neutral cholesterol ester hydrolase 1 is structurally and functionally conserved in *C. elegans*

In mammals, NCEH1 has been identified as the initial enzyme in reverse cholesterol transport in arteriosclerosis by converting the storage form, cholesterol ester, to the metabolically active form as free cholesterol. In *C. elegans*, the *nceh-1* gene encodes the worm homolog of this enzyme, termed NCEH-1; sharing 28% amino acid identity and 66% amino acid similarity with human NCEH1, as defined by the Clustal Omega software (Fig. 1A). Importantly, the His-Gly dipeptide motif and the GXSXG active serine motif of serine esterase, which are critical for hydrolase activity (26), are conserved in the *C. elegans* NCEH-1 amino acid sequence (boxes in Fig. 1A).

Increased NCEH activity diminishes the levels of cholesterol ester and free cholesterol in lipid-laden arterial smooth muscle cells *in vitro* (27) and cholesterol ester and free cholesterol accumulate *in vivo* in an *Nceh1* knockout mouse model (28). To investigate whether cholesterol ester hydrolysis is functionally conserved in *C. elegans*, we quantified total body cholesterol levels of wild type (WT) Bristol strain N2 worms treated with either empty vector (EV) control RNAi and *nceh-1* RNAi. When *nceh-1* was knocked down systemically in N2 worms, total cholesterol increased compared to EV control (Fig. 1B), demonstrating the conserved cholesterol ester hydrolysis activity of NCEH-1, consistent with mammalian models where deficient cholesterol ester hydrolase induces an accumulation of cholesterol ester and free cholesterol (28).

Human NCEH is localized at the ER with its N-terminal anchored to the membrane and catalytic and lipid-binding domains in the lumen (26). Nematode NCEH-1, with conserved catalytic and lipid-binding domains, may also involve in ER integration. We therefore measured the ER stress response in *C. elegans* using an established reporter strain that enables quantification of the expression of the *hsp-4* gene, which encodes the worm homolog of the ER chaperone BiP (P_{hsp-4}::GFP). A significantly enhanced ER stress response was displayed following systemic knockdown of *nceh-1* (Fig. 1C–E). This therefore asserts that NCEH-1 orchestrates ER function in *C. elegans*, consistent with a role in cholesterol metabolism where increased cholesterol level enhances ER stress in mice and human studies (29). This confirmation of NCEH-1 functional homology provides a basis for the following mechanistic studies.

NCEH-1 is protective against α-syn-induced DA neurodegeneration

We previously reported that NCEH-1 depletion by RNAi enhanced α-syn aggregation in *C. elegans* body wall muscle cells (14). Here, we wanted to extend this observation by examining α-syn toxicity in DA neurons. In *C. elegans*, overexpressing α-syn in DA neurons causes age- and dose-dependent neurodegeneration (30); at day 4, 69% of the population exhibited normal DA neurons, but at day 7, this was reduced to 45% (Fig. 2A). Knocking down *nceh-1* specifically in the DA neurons enhanced α-syn-induced neurotoxicity where only 39% and 15% of worms displayed normal DA neurons at days 4 and 7, respectively (Fig. 2A). A positive control RNAi was performed (*vps-41*) at days 4 and 7, and at day 7 knockdown of this endosomal gene product revealed significant neurodegeneration. RNAi knockdown was also performed in DA neurons that do not express α-syn and there was no significant difference between *nceh-1* depletion

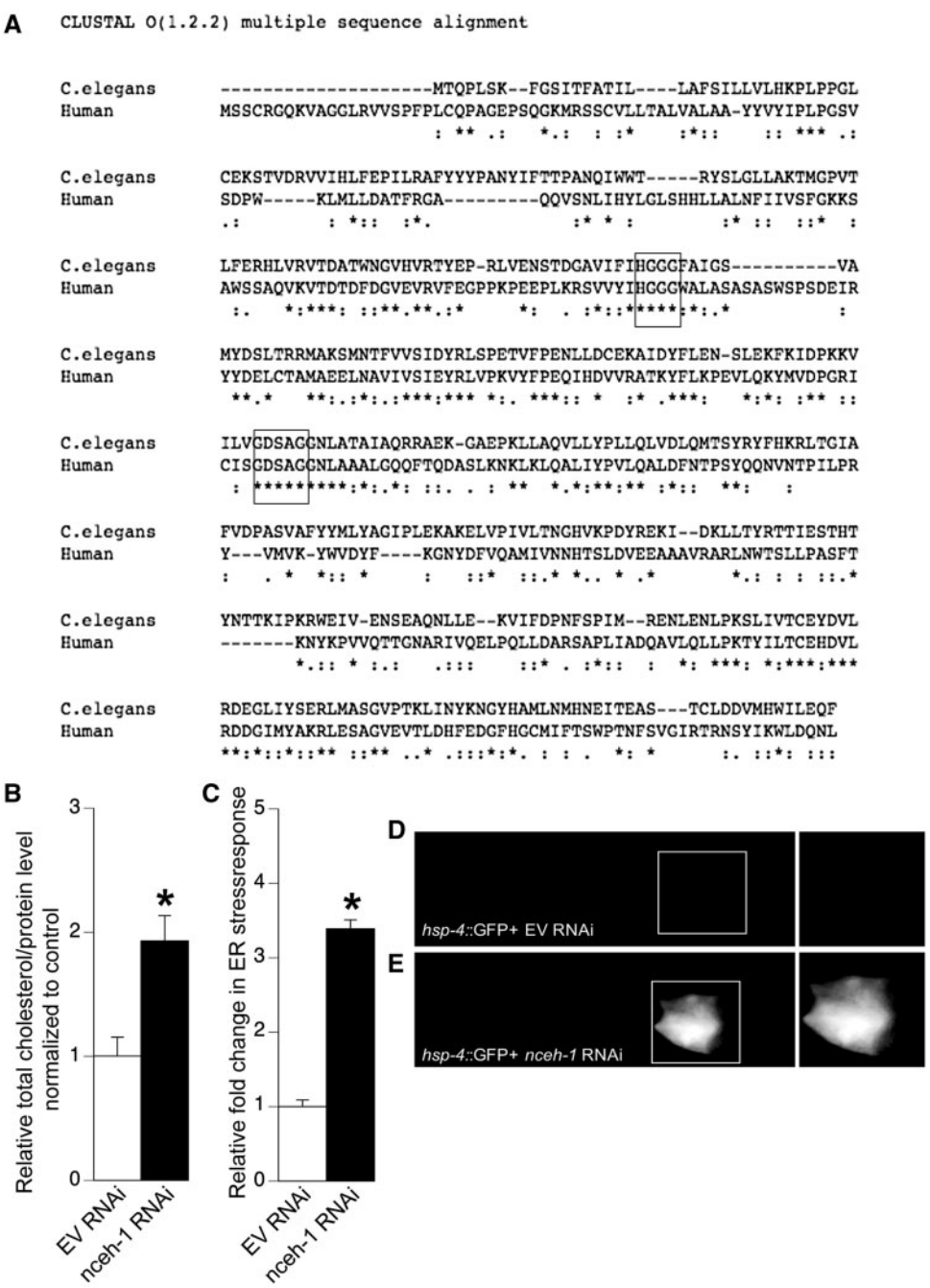

Figure 1. Conserved *C. elegans* NCEH-1 modulates cholesterol level *in vivo*. (**A**) Alignment of neutral cholesterol ester hydrolase in human and *C. elegans* where "*" indicates identity, whereas ":" indicates strong and "." weak similarity. The conserved hydrolytic sites are shown in boxes. (**B**) Normalized measurements of total cholesterol (free cholesterol + cholesterol ester) in day 4, N2 worms that were continuously exposed to RNAi bacteria containing EV or *nceh-1* dsRNA. This was a cholesterol oxidase procedure that was normalized to total protein. Knockdown of empty vector (EV) is a targeting control. (**C**) The relative fold change in ER stress in $P_{hsp\text{-}4}$::GFP worms exposed to EV or *nceh-1* dsRNA. (D, E) Fluorescent micrographs of *C. elegans* expressing the ER stress reporter $P_{hsp\text{-}4}$::GFP treated with EV (D) or *nceh-1* (E) RNAi. The white boxes indicate the anatomical region measured within all animals that consistently exhibits the highest levels of fluorescence intensity and is used to quantitate the change of ER stress by activation of HSP-4 (*C. elegans* BiP). Each bar represents the average of three independent experiments and data are represented as mean ± SEM. *$p<0.05$, one-way ANOVA with a Tukey post hoc test.

and EV knockdown (Fig. 2B). Thus, NCEH-1 promotes DA neuron health over time, in that progressive DA neurodegeneration by α-syn is enhanced by *nceh-1* depletion.

We further overexpressed the cDNA for *nceh-1* specifically within DA neurons to address whether NCEH-1 is sufficient to protect against α-syn-induced neurodegeneration. Overexpression of NCEH-1 under the *dat-1* (DA transporter) promoter significantly protected worms from α-syn neurotoxicity (Fig. 2C–E). Semi-quantitative RT-PCR confirmed that the transcription of α-syn did not change when *nceh-1* was overexpressed under this same promoter in the DA neurons (data not shown).

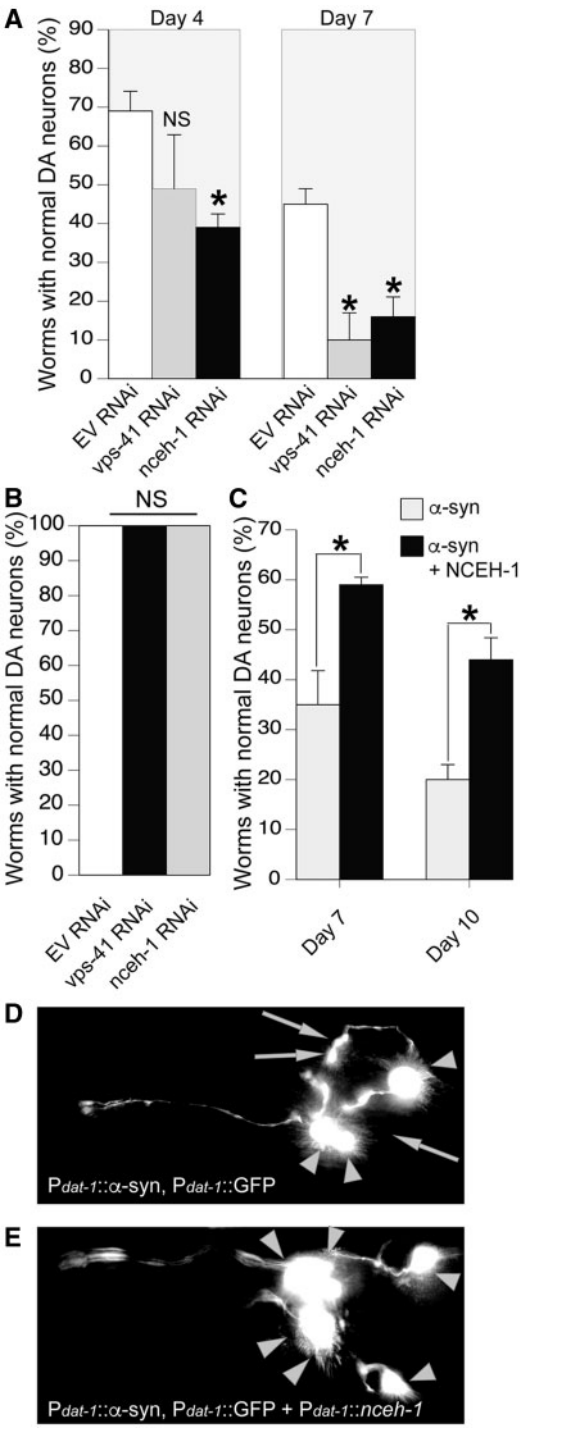

Figure 2. NCEH-1 is neuroprotective against α-syn-induced neurodegeneration. (**A**) Day 4 or 7 worms with intact DA neurons following EV, *vps-41* or *nceh-1* RNAi. *vps-41* knockdown is used as a positive control (52). RNAi knockdown was performed selectively the DA neurons of *sid-1* mutant worms expressing P_{dat-1}::*sid-1* + P_{dat-1}::α-syn + P_{dat-1}::GFP. (**B**) GFP only *sid-1* mutant worms expressing P_{dat-1}::*sid-1* + P_{dat-1}::GFP with wild type DA neurons following EV, *vps-41* or *nceh-1* RNAi at day 6. (**C**) Overexpression of NCEH-1 (P_{dat-1}:: *nceh-1* + P_{dat-1}::α-syn + P_{dat-1}:: GFP) rescues α-syn-induced neurodegeneration at days 7 or 10. (**D,E**) Representative images of the six anterior DA neurons in the head of α-syn (D) and α-syn worms overexpressing P_{dat-1}::*nceh-1* (E). Arrowheads indicate normal DA neuron cell bodies. Arrows show areas where DA neurons are degenerated in α-syn animals. Data are represented as mean ± SD. *$P < 0.05$, one-way ANOVA with a Tukey post hoc test (B) or two-way ANOVA with a Sidak post hoc test (A, C).

NCEH-1, as a downstream component in the IGF/insulin-like signaling pathway, has no effect on worm lifespan

Aging is the most prevalent risk factor for PD (31). In *C. elegans*, *daf-2* mutation is well-known for doubling lifespan (13). We identified *nceh-1* as a positive hit from a genetic screen for putative metabolic modulators at intersection of aging and neurodegeneration (14), whereby Murphy *et al.* showed that the *nceh-1* mRNA level was up-regulated in response to RNAi or mutation of *daf-2* by microarray analysis (15). We confirmed that the *nceh-1* mRNA level was altered in *daf-2(e1370)* mutant worms using quantitative real-time PCR (RT-qPCR). The results showed that there was a boost in the transcription of *nceh-1* in *daf-2* mutant animals compared to WT N2 worms (Fig. 3A). There are many downstream components of the IIS pathway; one of these is DAF-16/FOXO, which functions as a key regulator of many cytoprotective genes. We examined *nceh-1* transcriptional level in a *daf-2(e1370), daf-16(m26)* double mutation and discovered that, in this background, the increased transcription of *nceh-1* by *daf-2* mutation was only partially eliminated, indicating that *nceh-1* is a target gene downstream of the IIS pathway (Fig. 3A).

We previously reported that the *daf-2* mutation inhibits formation of misfolded α-syn protein in *C. elegans* body wall muscle cells and that knockdown of *daf-2* in DA neurons rescues the neuronal death caused by α-syn toxicity (14). Since *nceh-1* transcription is up-regulated in the *daf-2* mutant background, it is possible that the neuroprotection afforded by *daf-2* mutation is partially due to an increase of *nceh-1*. Likewise, we showed that *daf-2* knockdown in the DA neurons by RNAi also resulted in neuroprotection. However, simultaneous knockdown of both *nceh-1* and *daf-2* showed that the neuroprotective phenotype conferred by *daf-2* RNAi was reduced at an earlier stage and was eliminated during aging by *nceh-1* deficiency (Fig. 3B).

DAF-16 is a FOXO transcription factor downstream of DAF-2 and its phosphorylation when *daf-2* is suppressed plays a critical role in longevity by translocation to the nucleus where DAF-16 increases the expression of anti-stress genes (15). Previously, we have shown that knockdown of *nceh-1* failed to change DAF-16::GFP nuclear localization in *daf-2* mutant worms (14). To further explore the dependence of NCEH-1-mediated neuroprotection on DAF-16, we compared the combinatorial DA neuron-specific RNAi effect of *daf-16* + *nceh-1* to single RNAi of *nceh-1*. These results indicated that there was a synergistic effect on the enhancement of neurodegeneration by the double-knockdown, implying that DAF-16 may not be the sole factor regulating the neuroprotective role of NCEH-1 in modulating α-syn-induced toxicity (Fig. 3C).

Mutation of *daf-2* extends lifespan; therefore, we asked whether the neuroprotection associated with NCEH-1 was due to a developmental delay and postponed biological (vs. chronological) aging. Thus, we measured the lifespan of worms with either a neuronal or systemic alteration in *nceh-1* levels. Survival data displayed that overexpressing NCEH-1 in DA neurons (with α-syn) did not significantly impact the aging process (Fig. 3D). Additionally, systemic knockdown of *nceh-1* did not alter the longevity resulting from *daf-2* mutation (Fig. 3E). Consequently, we concluded that the neuroprotection exhibited by NCEH-1 was not due to an extension of lifespan.

Prolonged living does not assure extending the period and quality of healthier life. Healthspan is associated with an increased resilience to select pathogenic insults. As an established indicator of *C. elegans* healthspan, we examined the effect of *nceh-1* activity on survival against oxidative stress

induced by exposure to paraquat (N,N'-dimethyl-4,4'-bipyridinium dichloride) (32). A secondary assay was also employed to quantify movement deficits caused by oxidative stress. This entailed scoring thrashing behavior (body strokes in liquid) following an 8-h exposure of 100mM sodium azide (33). Both survival time and the number of body strokes following systemic knockdown of *nceh-1* (or EV) were counted, respectively, at distinct times, every 5 days until death. The results of these two healthspan assays revealed that oxidative stress-treated WT animals displayed a decline in both survival and movement with time and that reduction of NCEH-1 function significantly exacerbated these effects (Fig. 3F–G).

The hydrolase activity of NCEH-1 modulates neuroprotection

Since the neuroprotection afforded by NCEH-1 is not due to a delay of aging, we next hypothesized that its cholesterol ester hydrolytic activity might account for diminished α-syn toxicity. Two critical catalytic sites for the hydrolytic activity of NCEH were reported: the His-Gly dipeptide motif HGGG and GXSXG active serine motif (26). Amino acid substitution in either G114A or S191A can eliminate NCEH hydrolase activity in HEK293 cells, *in vitro* (19). Since these presumptive hydrolytic sites are conserved (Fig. 1A), we introduced these amino acid changes in worm NCEH-1 and expressed these variants in *C. elegans* DA neurons to investigate their impact on α-syn-induced neurodegeneration. Overexpression of G114A failed to protect against α-syn neurotoxicity while overexpression of S191A was significantly neuroprotective (Fig. 4A). When the double mutation of G114A and S191A was introduced into DA neurons in α-syn worms, the neuroprotection of NCEH-1 was eliminated (Fig. 4A). While the data from the S191A substitution seemingly contradicted that reported for an *in vitro* cell model, this distinction may reflect a functional difference within an *in vivo* context and/or the presence of α-syn in an *in vivo* and/or dopaminergic background.

Exogenous cholesterol enhances α-syn-induced neurodegeneration

Considering that knockdown of NCEH-1 increases cholesterol levels and enhances α-syn-induced neurodegeneration (Fig. 1B and 2A), we were curious to explore the effect of adding exogenous cholesterol on α-syn neurotoxicity. A concentration gradient of cholesterol was added to the growth medium for exposure to α-syn worms. Importantly, *C. elegans* do not naturally synthesize cholesterol, and it is typically an added fundamental component of standard worm growth media. We quantified the total cholesterol level in worms fed with different amounts of exogenous cholesterol. Although the addition of a high (50 μg/ml) level cholesterol seemed to exhibit a trend toward endogenous cholesterol accumulation, there was no significant difference in the total cholesterol level among animals with various concentrations of cholesterol exposure (Fig. 4B). In contrast, under conditions of standard cholesterol supplementation (5 μg/ml), 27% of α-syn transgenic worms displayed intact DA neurons, however, when the cholesterol level was reduced by 2.5 times (2 μg/ml), worms with normal DA neurons increased to 43%. In contrast, exposure to the higher concentration of cholesterol (50 μg/ml) significantly enhanced DA neurodegeneration, whereby only 17% of α-syn transgenic worms displayed normal DA neurons (Fig. 4C).

Though alteration in the amount of cholesterol added into the nematode growth medium failed to change the endogenous cholesterol stored in these animals, there is a significant difference of the cholesterol gradient on DA neuronal health. One thing to note is that total cholesterol is inclusive of both cholesterol ester and free cholesterol. Under normal conditions, cholesterol ester content is very low, comprising about 1% of total cholesterol (34). The detrimental effect of increasing cholesterol fed may result in an accumulation of cholesterol ester, for which a change is difficult to measure due to the limited content. Another explanation is that the processes which worms undergo to maintain cholesterol homeostasis enhance α-syn neurotoxicity. Alternatively, it seems that there is a trend of cholesterol level change in worms fed with 5 μg/ml and 50 μg/ml of cholesterol. Considering the critical role of cholesterol in living animals, even a subtle change might have a substantial functional impact. As a result, DA neurodegeneration is correlated with cholesterol exposure in α-syn expressing worms.

Depletion of cholesterol impairs neuroprotection by NCEH-1

If NCEH-1 prevents DA neurons from degenerating via a decrease of cholesterol, we hypothesized that limiting cholesterol levels in NCEH-1 overexpression worms would result in synergistic neuroprotection. Immediately at hatching, *C. elegans* larvae were exposed to growth medium either with or without cholesterol. Consistent with the previous cholesterol gradient result (Fig. 4C), at both day 7 and 10, α-syn control worms displayed more intact DA neurons without cholesterol (Fig. 4D). Furthermore, when cholesterol was removed, NCEH-1 neuroprotection was significantly reduced. For example, at day 10, the percentage of NCEH-1 overexpression worms displaying normal DA neurons when cholesterol was removed from the medium was equivalent to α-syn control worms with normal cholesterol (Fig. 4D). These data indicate that the NCEH-1 neuroprotection is dependent on the presence of cholesterol, especially in aged worms.

Having established that cholesterol is essential for neuroprotective activity of NCEH-1, we wanted to further evaluate a series of established mechanisms and modulators of cholesterol metabolism in the context of DA neurodegeneration. These include: cholesterol endocytosis, enzymatic regulation and efflux, as well as the role of cholesterol as a hormonal precursor and effector of mitochondrial function.

The role of cholesterol endocytosis in NCEH-1 neuroprotection

In further considering the requirement of cholesterol for NCEH-1-mediated neuroprotection, we examined the effect of cholesterol endocytosis on α-syn neurotoxicity. In *C. elegans*, LRP-2 is an ortholog of the low-density lipoprotein receptor-related protein 1 (LDLR), which receives LDL-cholesterol at the plasma membrane (34). Depletion of this gene significantly enhanced DA neurodegeneration (Fig. 4E). Further, when we knocked down *lrp-2* in DA neurons of worms overexpressing NCEH-1, this revealed that neuroprotection of NCEH-1 against α-syn was abolished (Fig. 4E). Collectively, cholesterol endocytosis contributes to neuroprotection from α-syn-induced degeneration; NCEH-1 functions downstream of cholesterol endocytosis and its neuroprotective role is dependent on LDLR.

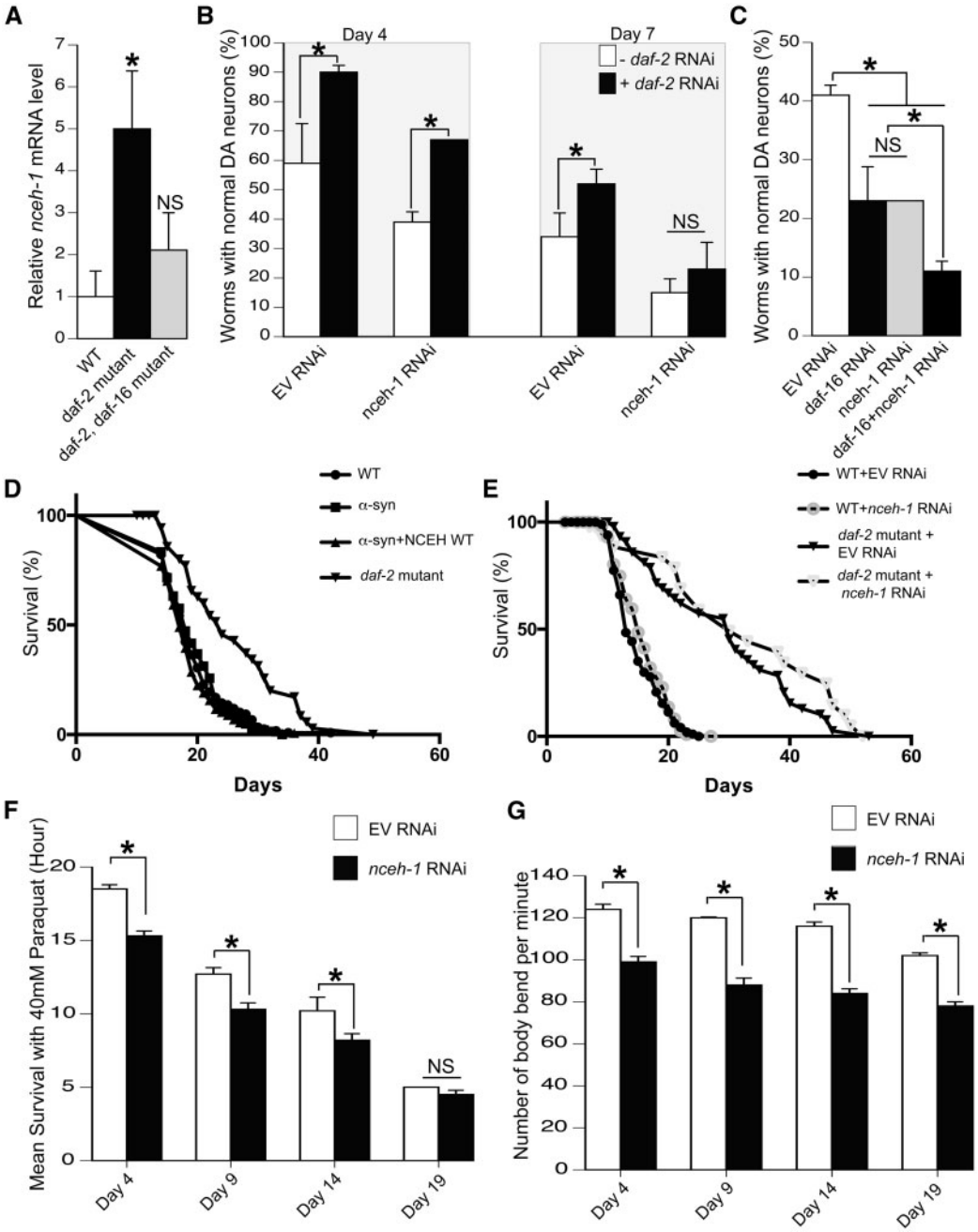

Figure 3. NCEH-1 acts downstream of DAF-2 and modulates healthspan but not lifespan. (**A**) Relative mRNA levels of *nceh-1* in WT, *daf-2* mutant and *daf-2*, *daf-16* double-mutant worms. (**B**) Day 4 or 7 worms with normal DA neurons following EV or *nceh-1* RNAi in *sid-1*; P_{dat-1}::*sid-1*; P_{dat-1}::α-syn; P_{dat-1}:: GFP worms with or without *daf-2* knockdown. (**C**) Worms with normal DA neurons after RNAi of EV, *daf-16*, *nceh-1* and *daf-16* + *nceh-1*, at day 6. (**D**) Survival analysis for WT, P_{dat-1}::α-syn, P_{dat-1}::α-syn + P_{dat-1}::*nceh-1* and *daf-2* worms. (**E**) Survival curves for *daf-2* mutant worms fed with EV or *nceh-1* dsRNA. (**F**) Median survival time of N2 worms with EV or *nceh-1* systemic RNAi exposed to 40mM paraquat. (**G**) The number of trashes per minute of WT worms treated with EV or *nceh-1* systemic RNAi. Data are represented as mean ± SD (A, B, C) and mean ± SEM (F, G). *$P < 0.05$, one-way ANOVA with a Dunnett post hoc test (A, C) or two-way ANOVA with a Sidak post hoc test (B, F, G). Survival was evaluated using a Mantel-Cox test (D-F).

Enzymatic inhibition of ACAT protects against α-syn toxicity

Cytosolic cholesterol pools are under a dynamic turnover between the free and esterified forms of cholesterol (35). Cholesterol ester entering cells as part of apoB-containing lipoproteins is known to be hydrolyzed by lysosomal acid lipase, leading that free cholesterol is available to enter various cellular pools. A fraction of free cholesterol trafficked to the ER is esterified by Acyl Co-A: cholesterol acyltransferase (ACAT). When potentially cytotoxic levels of free cholesterol are reached, ACAT activates to increase the formation of cholesterol ester as lipid droplets (36). The reciprocal synthesis and hydrolysis of cholesterol esters by ACAT and NCEH occur continuously to maintain this equilibrium, the impact of which has been noted in studies on atherosclerosis (37).

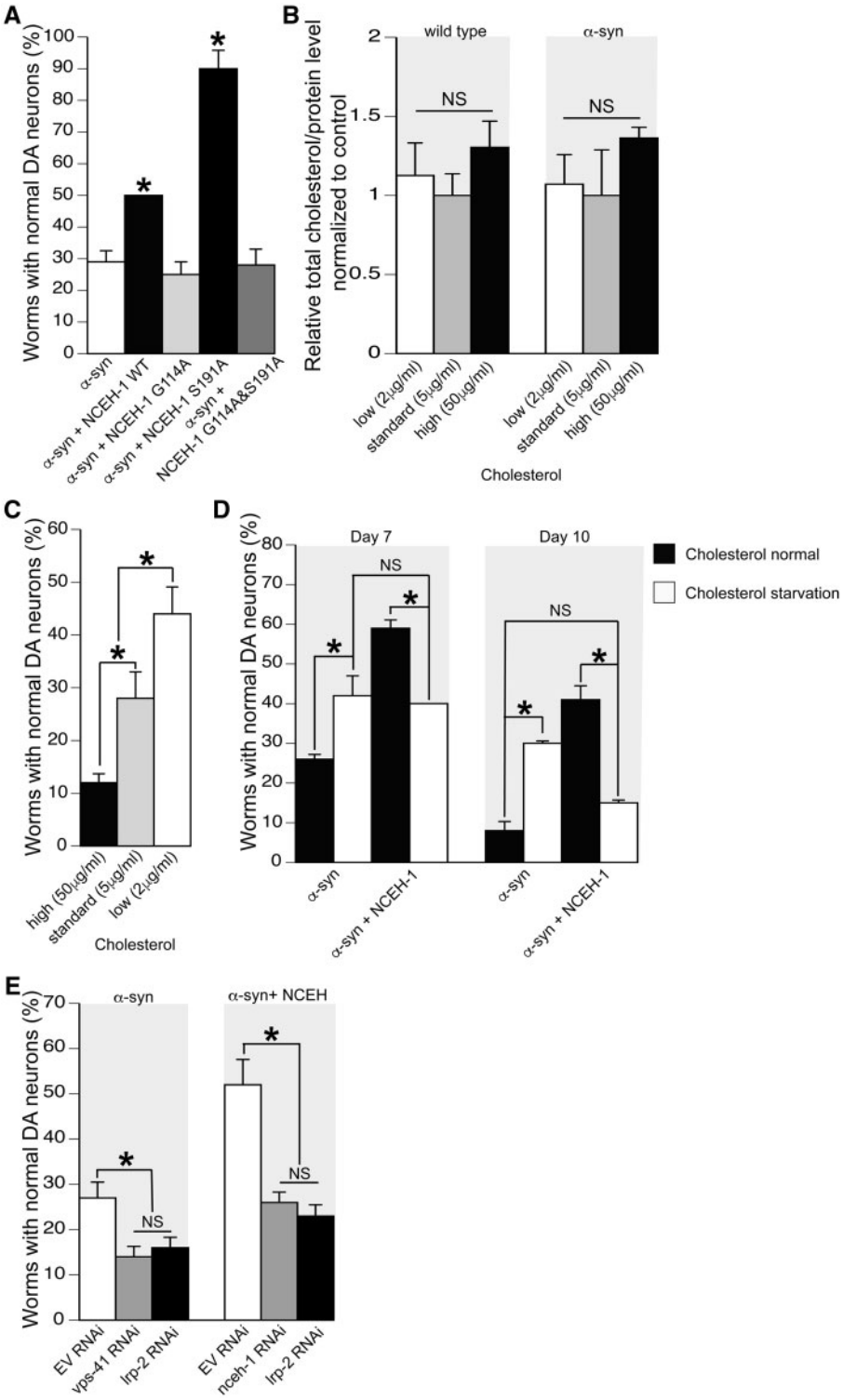

Figure 4. Cholesterol concentration, hydrolysis, and endocytosis into DA neurons are critical to NCEH-1 neuroprotection. (**A**) Comparison of worm populations with normal DA neurons among $P_{dat\text{-}1}$::α-syn; $P_{dat\text{-}1}$::GFP worms with or without various NCEH-1 overexpression variants analyzed at day 7 after hatching. (**B**) Normalized measurements of total cholesterol normalized to total protein in day 4, wild type and α-syn worms exposed to either 50, 5 or 2 μg/ml cholesterol. (**C**) $P_{dat\text{-}1}$::α-syn; $P_{dat\text{-}1}$::GFP worms with normal DA neurons following exposure to either 50, 5 or 2 μg/ml cholesterol and analyzed at day 7 after hatching. (**D**) Day 7 or 10 $P_{dat\text{-}1}$::α-syn; $P_{dat\text{-}1}$::GFP worms with or without $P_{dat\text{-}1}$::*nceh-1* were treated with either a standard concentration of cholesterol (5 μg/ml) or no cholesterol. (**E**) *sid-1*; $P_{dat\text{-}1}$::α-syn; $P_{dat\text{-}1}$::GFP worms with normal DA neurons following RNAi knockdown using EV or *lrp-2* dsRNA in the absence or presence of $P_{dat\text{-}1}$::*nceh-1* at day 7. Data are represented as mean ± SD. $^*P < 0.05$, one-way ANOVA with a Dunnett post hoc test (A), Tukey post hoc test (C), or two-way ANOVA with Sidak post hoc test (B, D, E).

In *C. elegans*, *mboa-1* encodes an Acyl Co-A:cholesterol acyltransferase homolog. We discerned that RNAi knockdown of *mboa-1* selectively in DA neurons resulted in enhanced α-syn-induced neurodegeneration (Fig. 5A). Furthermore, knockdown of *mboa-1* in the DA neurons of worms overexpressing NCEH-1 failed to increase the neuroprotection by NCEH-1 (Fig. 5A). Therefore, sufficient cholesterol ester as the substrate of NCEH-1 is a prerequisite for neuroprotection.

The ACAT inhibitor, Sandoz 58035, was also examined in *C. elegans* expressing α-syn in DA neurons. Following a dose-response study, we discerned that concentrations of 25–75 μg/ml of the ACAT inhibitor significantly increased the number of worms with normal DA neurons (Fig. 5B). However, a threshold was reached at 100 μg/ml ACAT inhibitor whereby this concentration substantially lowered DA neuron survival (Fig. 5B), as was observed by *mboa-1* knockdown in DA neurons (Fig. 5A). These data led to the conclusion that the interplay of NCEH-1 and ACAT modulation of cholesterol ester/free cholesterol formation exhibits a potentially "tunable" mechanism to attenuate α-syn toxicity in DA neurons.

Cholesterol efflux is critical to NCEH-1 neuroprotection

Neurons can store, but not degrade cholesterol. Excessive cellular cholesterol needs to be removed in the form of free cholesterol. Hydrolysis of cellular cholesterol ester is considered the rate-limiting step in free cholesterol efflux (38,39). Cholesterol ester hydrolase activity not only reduces cellular accumulation of cholesterol esters but also enhances cholesterol efflux in human THP1 macrophages (40). The ATP-binding cassette ABC transporter ABCA1, which is located primarily at the plasma membrane, plays a critical role in cholesterol efflux. In *C. elegans*, we determined that the DA neuron-specific knockdown of the homolog of mammalian ABCA1, *abt-2*, enhanced neurodegeneration caused by α-syn (Fig. 5C). Moreover, NCEH-1 neuroprotection was significantly reduced when *abt-2* was deficient. Consequently, the block of cholesterol efflux in DA neurons by knockdown of the ABC transporter impairs the neuroprotection of NCEH-1.

Estradiol rescues enhanced neurodegeneration caused by *nceh-1* knockdown

Cholesterol is an obligate precursor for all steroid hormones. Estradiol (E2) is the most effective form of estrogen, which has been purported to serve in a protective capacity against PD in women (41). Therefore, we examined the effect of E2 in the context of enhanced α-syn neurotoxicity caused by *nceh-1* knockdown. Worms were exposed to E2 (or solvent control) in the media from hatching. E2 (at a concentration of 10^{-8} M) did not provide significantly protection to DA neurons from α-syn worms treated with EV dsRNA (Fig. 6A). In contrast, when α-syn worms were treated with *nceh-1* dsRNA, there was significant rescue by E2, whereby the average percentage of worms with intact DA neurons increased from 13% to 47% (Fig. 6A). Thus, E2 might counterbalance the impact of cholesterol ester accumulation in DA neurons; this may reflect a compensatory hormonal strategy utilized in states of cholesterol imbalance.

NCEH-1 modulates mitochondrial ROS levels through cholesterol metabolism

The formation and excretion of oxysterols, such as E2, are accounted for by the maintenance of cholesterol homeostasis

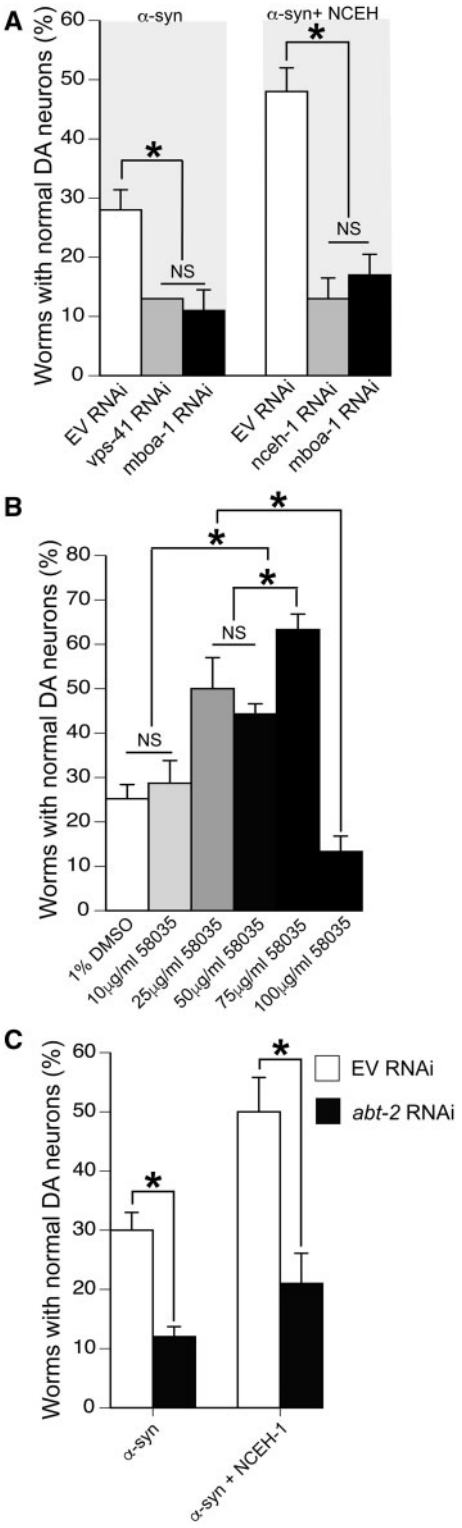

Figure 5. The storage and efflux of cellular cholesterol modulate NCEH-1 neuroprotection. (**A**) *sid-1*; P_{dat-1}::α-syn; P_{dat-1}::GFP worms with normal DA neurons following RNAi knockdown of EV or *mboa-1* in the absence or presence of P_{dat-1}::*nceh-1* at day 7. (**B**) P_{dat-1}::α-syn; P_{dat-1}::GFP worms with normal DA neurons after exposure to the ACAT inhibitor, Sandoz 58035, at day 7. (**C**) *sid-1*; P_{dat-1}::α-syn; P_{dat-1}:: GFP worms with normal DA neurons at day 7 following EV or *abt-2* RNAi with or without the overexpression of P_{dat-1}::*nceh-1*. Data are represented as mean ± SD. *$P < 0.05$, one-way ANOVA with Dunnett post hoc test (B) or two-way ANOVA with Sidak post hoc test (A, C).

when free cholesterol is liberated from stored ester (42). In *C. elegans*, the E2 precursor, pregnenolone, is synthesized from cholesterol in the mitochondria and acts as the substrate for all other steroid hormones. Thus, mitochondria are a "first stop" for metabolically active cholesterol. Using an *ex vivo* assay, 2′,7′-dichlorofluorescein diacetate (DCF-DA) fluorescence in whole worms, we discovered that *nceh-1* overexpression in DA neurons diminished mitochondrial ROS levels in α-syn worms (Fig. 6B). Together, these findings suggest that NCEH-1 activity in DA neurons may participate in lowering mitochondrial stress caused by α-syn.

Discussion

The functional relationship between sterol metabolism and neurodegeneration has long been a source of intrigue for scientists. This is heightened when considering the known risk factors for these diseases of aging, such as obesity, sex-specific distinctions in disease susceptibility, as well as the potential effects and prevalence of cholesterol-modifying drugs (*i.e.* statins) prescribed for use in human populations. In this regard, a more mechanistic understanding of the enzymatic regulators and modulators of the distinct cellular states of cholesterol is required. Furthermore, it is now clear that we need to understand how cholesterol and its modulators impact *in vivo* dynamics in response to established disease-associated stressors of proteostasis and neuronal survival (*i.e.* α-syn).

Here we provide evidence of a functional role for NCEH-1 in regulating a cholesterol-associated mechanism of protection against α-syn-induced neurodegeneration in DA neurons. Using a suite of bioassays that take advantage of the genetic attributes of *C. elegans* to rapidly probe mechanistic features of neurodegeneration *in vivo*, we revealed that NCEH-1 neuroprotection against α-syn toxicity based on its enzymatic regulation of cholesterol metabolism. Deficient NCEH-1 activity resulted in an accumulation of cellular cholesterol, which was shown harmful to neuronal health with α-syn. Moreover, the presence of cholesterol and its internalization by membrane LDLRs are essential to the neuroprotection of NCEH-1. However, addition of excessive exogenous cholesterol deteriorates DA neuron health. Concomitantly, we determined that sufficient cholesterol efflux is critical to the NCEH-1 neuroprotection which liberates cholesterol from a storage form. Addition of the steroid hormone estradiol can effectively rescue the enhanced neurodegeneration caused by *nceh-1* knockdown. Lastly, NCEH-1 can also attenuate mitochondrial stresses caused by α-syn toxicity.

In Figure 6C, we summarized the features of neuronal cholesterol metabolism investigated in this study. NCEH is depicted as localized to the ER, where cholesterol conversion occurs. To further delineate the neuroprotective nature of NCEH-1, we investigated four distinct aspects of cholesterol metabolism in this context: 1) LDLR-mediated endocytosis; 2) cytosolic storage as cholesterol ester by ACAT; 3) synthesis of oxysterols initiated in mitochondria; 4) and cholesterol efflux. These mechanistic studies revealed that the cholesterol endocytosis pathway was required for prevention of α-syn toxicity because neuroprotection of NCEH-1 is dependent on LDLR.

A retrograde plasma membrane to ER cholesterol trafficking pathway has been reported (43,44). This enables cholesterol to arrive at the ER without vesicles. However, it is unclear how LDLR regulates retrograde cholesterol trafficking. Results from an *in vitro* cholesterol monitoring assay showed that it takes about 30 min for exogenous cholesterol to become available for efflux at the plasma membrane. Relatively speaking, cholesterol

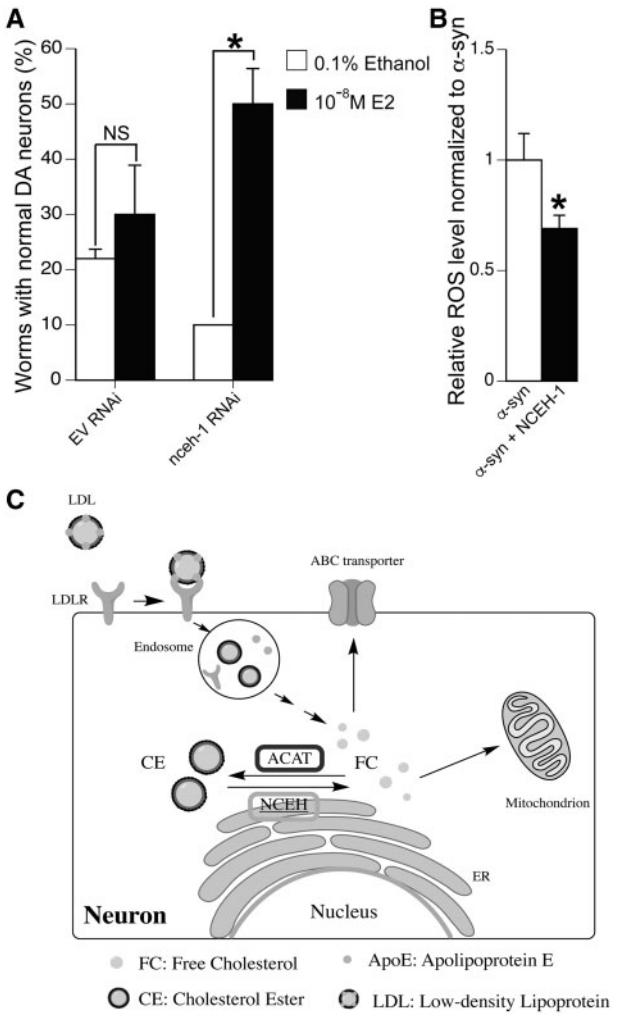

Figure 6. The effect of NCEH-1 on mitochondrial stress and a depiction of cellular features of cholesterol metabolism. (**A**) $P_{dat\text{-}1}$:: α-syn; $P_{dat\text{-}1}$:: GFP worms exposed to EV or *nceh-1* dsRNA with treatment of 10^{-8} M estradiol (or 0.1% ethanol control) at day 7 after hatching. (**B**) The relative ROS level as indicated by DCF-DA assay in $P_{dat\text{-}1}$::α-syn; $P_{dat\text{-}1}$::GFP and $P_{dat\text{-}1}$::α-syn; $P_{dat\text{-}1}$::*nceh-1* worms. Data are represented as mean ± SD. *$P < 0.05$, two-way ANOVA with Sidak post hoc test (A) or Student's *t*-test (B). (**C**) A sketch of cholesterol metabolism in neurons. Cholesterol uptake is via LRP-2/LDLR-mediated endocytosis in the form of cholesterol ester. It is then liberated to free cholesterol in lysosome. Excess free cholesterol is converted to esterified cholesterol ester by ACAT and stored as lipid droplets. Free cholesterol can also be released from neurons through ABT-2/ABCA1-associated cholesterol efflux or initiating conversion to oxysterols at mitochondria. NCEH can release free cholesterol from stored lipid droplets and serves as a rate-limiting enzyme for cholesterol efflux.

esterification in the ER takes double or triple this time (45). Thus, there may be excess cholesterol to efflux rather than esterify, particularly with increased NCEH-1 activity. Alternatively, cholesterol transport to the plasma membrane or ER may be carried out by different mechanisms. The overexpression of NCEH-1 may increase the release of free cholesterol from lipid droplets to synthesize a variety of oxysteroids [*i.e.* 24(S)-hydroxycholesterol, 22(R)-hydroxycholesterol, 24(S), 25-epoxycholesterol, and 27-hydroxycholesterol] (46). It is of note that when 24(S)-hydroxycholesterol is released from neurons, it can be taken up by surrounding glia. Interestingly, the binding of 24(S)-hydroxycholesterol with LXR, the Liver X vitamin-D-like nuclear hormone receptor, activates the ABCA1 transporter in neuroglia, triggering

an increased load of cholesterol from glia to neurons. As the *C. elegans* homolog of LXR is DAF-12, another established effector of longevity, it is possible that the overexpression of NCEH-1 might act as an "engine" to maintain cholesterol "flow" and homeostasis.

Cholesterol has been reported to interact with α-syn via its 3β-OH (47). Interestingly, a 3β-OH group exists in free cholesterol and E2/pregnenolone. Thus, the binding of cholesterol with α-syn may contribute to NCEH-1 neuroprotection. When overexpressed, NCEH-1 promotes the cellular free cholesterol mobilization, whose binding with α-syn may reduce cellular stress caused by the accumulation of α-syn in our tentative model of "cholesterol flow." Alternatively, NCEH-1 may promote α-syn departure from mitochondria as α-syn-binding pregnenolone leaves mitochondrial to restore normal mitochondrial function and decreases cellular oxidative stress (48,49). Notably, estrogen has been reported as an activator to NCEH activity in an atherogenesis mouse model (50).

Increased NCEH activity has been reported to diminish cellular cholesterol levels (28). Together with our findings, the effect of hydrolase activity on cellular cholesterol regulation is critical for NCEH-1 neuroprotection. The hydrolase-dead mutations, G114A and G114A + S191A, presumably eliminated cholesterol ester hydrolase activity and failed to protect against α-syn neurotoxicity. However, in the case of the S191A mutation, we observed a surprising increase in DA neuroprotection. In cholesterol ester hydrolysis, the glycine residues of NCEH-1 are important in stabilizing the reaction and in maintaining the substrate in place. Thus, glycine substitution in the hydrolase-dead mutation G114A suppresses NCEH-1 hydrolytic activity of through a partition of esterified cholesterol from the enzyme, failing to alter cholesterol metabolism in DA neurons. The catalytic serine residue initiates the nucleophilic attack on the carbonyl carbon of the ester bond. Free cholesterol is released after this step and NCEH-1 becomes acylated due to the covalent link between the acid moiety of cholesterol ester and the serine residue. It has been reported that such a serine-to-alanine substitution increases the biological activity of photochrome A *in vivo* (51). The S191A substitution may extend the predicted α-helix toward the amino terminus of the molecule, thereby facilitating and/or stabilizing conformational changes. Structural changes aside, the amino acid substitutions also increase the hydrophobicity of the amino-terminal domain, which may lead to the observed increase in biological activity. Serendipitously, the S191A variant of NCEH-1 could have therapeutic value for PD.

Finally, although *nceh-1* expression is regulated by DAF-2 (15), it does not influence lifespan. Moreover, its neuroprotective capacity is only partly suppressed by mutation in the gene encoding the FOXO transcription factor, DAF-16. This reflects a distinction between regulators of lifespan vs. healthspan, and that a divergence in downstream signaling from DAF-2 exists in mediating neuronal response to pathogenic stressors like α-syn. Taken together, our findings reveal a novel neuroprotective activity of NCEH-1 in attenuating dopaminergic neurodegeneration. Furthermore, this highlights the prospects for new disease-modifying interventions for PD that target the regulation of cholesterol metabolism in the nervous system.

Experimental Procedures

Plasmid construction

nceh-1 was amplified using cDNA as a template by Phusion high-fidelity polymerase (ThermoFisher). The cDNA was synthesized from total RNA extracted from day 4 N2 Bristol nematodes as described (52). An HA tag was added to the N-terminal of *nceh-1* cDNA during the PCR amplification. Using Gateway cloning (Life Technologies), PCR products were cloned into plasmid entry vector pDONR221 via a BP reaction and the entry clone further recombined into the Gateway pDEST-DAT-1 destination vector (53). To construct the point mutants of *nceh-1*, TagMaster site-directed mutagenesis kit (GM Biosciences) was used. The double-mutant plasmid was constructed by PCR-amplification using S191A primers based on G114A plasmid as templates. The sequences of these plasmids were verified by DNA sequencing. Primers were designed as follows:

nceh-1 Gateway forward: ggggacaagtttgtacaaaaaagcaggctc catgtatccttatgatgttcctgattatgctatgacacaaccattatccaaatttg

nceh-1 Gateway reverse: ggggaccactttgtacaagaaagctgggtc ttaaaattgctccaaaatccagtg

nceh-1 G114A forward: gccgtgatctttattcatgCcgggggatttgcg

nceh-1 G114A reverse: cgcaaatccccccgGcatgaataaagatcac ggc

nceh-1 S191A forward: ggtgatacttgtcggagatGctgctggcggaa atttg

nceh-1 S191A reverse: caaatttccgccagcagCatctccgacaagt atcacc

C. elegans strains

Nematodes were maintained using standard laboratory procedures (54). Polystyrene Petri dishes were used (item numbers: T3308 & T3501, VWR). The following strains were provided by the Caenorhabditis Genetics Center, CB1370 (*daf-2(e1370)* III), DR128 (*dpy-1(e1) daf-2(e1370)* III), DR1309 (*daf-16(m26)* I; *daf-2(e1370)* III), SJ4005 (*zcIs4* [P_{hsp-4}::GFP] V). The following strains UA44 (*baIn11* [P_{dat-1}::α-syn, P_{dat-1}::GFP]), UA196 (*sid-1(pk3321)*; *baIn33* [P_{dat-1}::*sid-1*, P_{myo-2}::mCherry]; *baIn11*] and UA286 (*baIn36* [P_{dat-1}::*sid-1*, P_{myo-2}::mCherry]; *vtIs7* [P_{dat-1}::GFP]) were generated as described previously (55,56). Both UA196 and UA286 express GFP, and SID-1 in the DA neurons under the *dat-1* promoter. Expression of *sid-1* enhances RNAi sensitivity in these neurons. UA196 additionally expresses α-syn in these neurons. Three independent stable transgenic lines were generated by injecting P_{dat-1}::*nceh-1* cDNA, along with a phenotypic *rol-6* marker into UA44 or UA196 hermaphrodites (UA289 (*baEx170*) and UA290 (*baEx171*), respectively). The roller phenotype is an indicator for the transgene presence. Point mutations of *nceh-1* (G114A, S191A and G114A + S191A) were made in the cDNA under the same P_{dat-1} promoter and injected into UA44 with *rol-6* marker to generate UA291 (*baEx172*), UA292 (*baEx173*) and UA293 (*baEx174*), respectively.

C. elegans chemical, steroid, and cholesterol exposure paradigms

Paraquat and sodium azide were dissolved in M9 buffer to a final concentration of 40mM and 100mM, respectively. Worms were exposed to paraquat till death and were treated with sodium azide 24 h before trashing analysis. ACAT inhibitor, Sandoz 58-035 (Sigma-Aldrich) was dissolved in dimethyl sulfoxide (DMSO) and sterilized by filtering through membranes with 0.2 μm pore sizes. 10, 25, 50, 75 and 100 μg/ml Sandoz 58-035 were added to 35-mm petri dishes containing preautoclaved media. DMSO solvent was kept at 1% among concentration

gradients. *C. elegans* were exposed to Sandoz 58-035 for 7 days before neuron scoring. E2 (Sigma-Aldrich) was treated to worms in a similar way at a final concentration of 10^{-8} M in 0.1% ethanol.

RNA interference treatments

All bacteria for RNAi were obtained from the Ahringer *C. elegans* library (57); they were isolated and grown overnight at 37 °C in LB media containing 100 μg/ml ampicillin. NGM plates containing 1mM IPTG were seeded with 250μl of RNAi culture and allowed to dry overnight. Six L4-stage worms were transferred on corresponding RNAi plates to lay eggs overnight at 20 °C. The offspring worms were continuously fed with bacteria containing dsRNA and transferred to corresponding fresh plates as needed to avoid starvation. For double RNAi, knock-down of two genes (*daf-16* + *nceh-1*) was performed by feeding an equal concentration mixture of each bacterial strain (as determined by OD_{600}) that each encoded for the expression of one dsRNA species (58).

C. elegans neurodegeneration analysis

Worms were analyzed for DA neurodegeneration as previously described (53). Briefly, synchronized worms were grown at 20 °C and scored by fluorescent microscopy (Nikon Eclipse E800) for DA neuronal survival indicated by GFP at day 4, 6, 7 or day 10 after hatching. Worms were considered normal when all six anterior DA neurons (four CEPs and two ADEs) were present without any visible signs of degeneration such as blebbing of processes or cell body rounding and/or loss. In total, at least 90 (30 in triplicate) adult worms were analyzed for each independent transgenic line or RNAi treatment. A Cool Snap CCD camera (Photometrics) driven by MetaMorph software (Molecular Devices) was used to acquire representative images. Statistics were analyzed using one-way ANOVA followed by Tukey post hoc test or two-way ANOVA with a Sidak post hoc test (GraphPad Prism software).

Cholesterol quantification assay

Cholesterol quantification was performed as previously described (59). Synchronized N2 worms were treated with systemic *nceh-1* or EV knockdown and harvested at day 4 after hatching. After thawing out from −80 °C, worm cuticles were broken down by 30s-sonification. 200μl of chloroform: isopropanol: NP40 (7:11:0.1) was added to each sample and the organic phase was transferred to a new tube for drying. Dried lipids were dissolved by 200μl cholesterol assay buffer provided in the cholesterol quantification kit (Sigma). 50μl of each sample was transferred in a black 96-well plate to be used in a microplate reader (BioTek). The amount of fluorometric (λ_{ex}= 535/λ_{em}= 587 nm) products was used to calculate total cholesterol via a standard curve achieved from standard lipids. Before the lipid extraction, 30 μl aliquots from each replicate were used for BCA protein quantification (Abcam) where the protein concentration for each sample was calculated using the BSA-standard curve by a colorimetric (562 nm) product (60). The result was the readout of total cholesterol normalized to protein level; the assay was repeated three times. Statistics were analyzed using unpaired Student's t-test.

Measurement of transcription by RT-qPCR

qPCR was used to verify the increase of *nceh-1* transcription in *daf-2* mutant worms. qPCR primers (forward: gagaactcgacggatggag; reverse: acagtttccggggacaatc) showed an efficiency of 95.7%. Synchronized young adult worms were collected at day 4 after hatching. Total RNAs were isolated as described previously (30). cDNAs were synthesized using iScript cDNA synthesis kit (Bio-Rad) and RT-qPCR reactions were performed using IQ SYBR Green Supermix (Bio-Rad) with the CFX96 Real-Time System (Bio-Rad) as described previously (52). Statistics were analyzed using one-way ANOVA followed by Tukey post hoc test.

Lifespan assay

Lifespan was assessed by the Cohort survival assay (61). At least 120 synchronized worms were grown at 20 °C and monitored for the occurrence of death or censored events every day until all worms were dead. We counted dead worms as "1". When worm bagging, vulva protrusion or uncoordinated movement was observed, those worms were censored and recorded as "0". Statistics were determined using Coherent survival analysis followed by Mantel-Cox test and two-way ANOVA with a Sidak post hoc test (GraphPad Prism).

Healthspan assay

In this assay, WT worms were synchronized at L1 stage and were transferred onto medium containing HT115 bacteria with EV or *nceh-1* dsRNA. Worms were transferred as needed to avoid starvation and were incubated at 20 °C to ensure at least 30 animals per treatment were present at the day of analysis. For the test of resistance of oxidative stress (32), every 5 days after adulthood, worms were transferred into a 96-well plate and soaked in 100μl of 40mM paraquat dissolved with M9 buffer. Every hour, worms were analyzed for the survival: if worms were straightened out with no response to a sudden strong light and eye-lash pick touch, we considered this as dead and scored "1" in contrast to alive worms score as "0". Mean survival was measured by Coherent survival analysis followed by Mantel-Cox test. For the trashing assay (62), worms were transferred into 35mm worm plates containing 100mM sodium azide solution for 8 h prior to analysis at day 4, 9,14 and 19. Digital videos of animal movement were acquired for 1 min using a Worm Tracker (MBF Biosciences). The thrashing frequency of the animals was quantified by counting body bends, defined as a change in direction of bending at the middle of worm body (33). The differences in oxidative stress resistance between RNAi treatments were compared using two-way ANOVA with a Sidak post hoc test (GraphPad Prism).

Measurement of ROS by using 2',7'-dichlorofluorescein diacetate (DCF-DA)

This assay was conducted as described previously (63). 50μM DCF-DA (Molecular Probes) was used in PBST to incubate with worm lysates from about 1000 day 4 worms for 2 h. Every 20 min, the microplate reader (BioTek) was programmed to read the fluorometric level at the excitation wavelength 485 nm and the emission wavelength 535 nm. We measured the fluorescence every 20 min for 2.5 h. Since the time-dependent increase in the fluorescence was linear over this timeframe, we used fluorescence intensity at 2.5 h for our analysis. Fluorescence intensity was normalized by subtracting the background

fluorescence of 250 μM DCF-DA solution in PBST at 1 h. 10 μl of worm lysates were used for protein quantification by BCA assay. Statistics were analyzed using unpaired Student's *t* test (GraphPad Prism).

ER stress assay

ER stress response was examined in *hsp-4*::GFP worms (64) which were fed with EV or *nceh-1* dsRNA. At late L4-stage, animals were mounted on a 2% agarose pad with 25mM levamisole. Using a Nikon E800 microscope with a CCD camera (Photometrics CoolSnap HQ) at 40× magnification, GFP intensity was measured in pixels and assigned arbitrary units (a.u.) from a 100 × 100 μm region of the anterior-most region of the intestine was detected by MetaMorph software (Molecular Devices Corp.). For each strain and condition, at least 30 animals were quantitated in three independent replicates. For each assay, the data presented are the normalized fold change mean ± SEM of three independent trials for every RNAi condition. Normalization compares GFP intensity for all the samples (*hsp-4*::GFP with EV or *nceh-1* RNAi) divided by the average of EV RNAi. Statistics were analyzed using unpaired Student's *t* test (GraphPad Prism).

Acknowledgements

We are grateful to all members of the Caldwell lab for their collegiality and teamwork. Special thanks to Laura Berkowitz for her invaluable contributions and Anthony Gaeta for generating some of the transgenic animals used in this work. Some strains were provided by the Caenorhabditis Genetics Center (CGC), which is funded by the NIH Office of Research Infrastructure Programs (P40 OD010440). GAC was supported by a grant from the National Institutes of Health (R15 NS075684-01). Additional support for SAG came from The University of Alabama College of Arts & Sciences Undergraduate Creative Activity and Research Academy.

Conflict of Interest statement. None declared.

Funding

National Institutes of Health (R15 NS075684-01) to GAC, University of Alabama College of Arts & Sciences Undergraduate Creative Activity and Research Academy.

References

1. Mauch, D.H., Nägler, K., Schumacher, S., Göritz, C., Müller, E.C., Otto, A. and Pfrieger, F.W. (2001) CNS synaptogenesis promoted by glia-derived cholesterol. *Science*, **294**, 1354–1357.
2. Hu, G., Antikainen, R., Jousilahti, P., Kivipelto, M. and Tuomilehto, J. (2008) Total cholesterol and the risk of Parkinson disease. *Neurology*, **70**, 1972–1979.
3. Gudala, K., Bansal, D. and Muthyala, H. (2013) Role of serum cholesterol in Parkinson's disease: A meta-analysis of evidence. *J. Parkinsons. Dis.*, **3**, 363–370.
4. Fernandez, H.H. (2015) 2015 Update on Parkinson disease. *Cleve. Clin. J. Med.*, **82**, 563–568.
5. Miyake, Y., Tanaka, K., Fukushima, W., Sasaki, S., Kiyohara, C., Tsuboi, Y., Yamada, T., Oeda, T., Miki, T., Kawamura, N. *et al.* (2011) Lack of association of dairy food, calcium, and vitamin D intake with the risk of Parkinson's disease: a case-control study in Japan. *Parkinsonism Relat. Disord.*, **17**, 112–116.
6. Bousquet, M., St-Amour, I., Vandal, M., Julien, P., Cicchetti, F. and Calon, F. (2012) High-fat diet exacerbates MPTP-induced dopaminergic degeneration in mice. *Neurobiol. Dis.*, **45**, 529–538.
7. Bosco, D.A., Fowler, D.M., Zhang, Q., Nieva, J., Powers, E.T., Wentworth, P., Lerner, R.A. and Kelly, J.W. (2006) Elevated levels of oxidized cholesterol metabolites in Lewy body disease brains accelerate alpha-synuclein fibrilization. *Nat. Chem. Biol.*, **2**, 249–253.
8. Marwarha, G. and Ghribi, O. (2015) Does the oxysterol 27-hydroxycholesterol underlie Alzheimer's disease-Parkinson's disease overlap?. *Exp. Gerontol.*, **68**, 13–18.
9. Tschäpe, J.A., Hammerschmied, C., Mühlig-Versen, M., Athenstaedt, K., Daum, G. and Kretzschmar, D. (2002) The neurodegeneration mutant löchrig interferes with cholesterol homeostasis and Appl processing. *embo J.*, **21**, 6367–6376.
10. Zhu, M. and Fink, A.L. (2003) Lipid binding inhibits α-synuclein fibril formation. *J. Biol. Chem.*, **278**, 16873–16877.
11. Wang, S., Zhang, S., Liou, L.-C., Ren, Q., Zhang, Z., Caldwell, G.A., Caldwell, K.A. and Witt, S.N. (2014) Phosphatidylethanolamine deficiency disrupts α-synuclein homeostasis in yeast and worm models of Parkinson disease. *Proc. Natl. Acad. Sci. U. S. A*, **111**, E3976–E3985.
12. Cohen, E. and Dillin, A. (2008) The insulin paradox: aging, proteotoxicity and neurodegeneration. *Nat. Rev. Neurosci.*, **9**, 759–767.
13. Kenyon, C., Chang, J., Gensch, E., Rudner, A. and Tabtiang, R. (1993) A *C. elegans* mutant that lives twice as long as wild type. *Nature*, **366**, 461–464.
14. Knight, A.L., Yan, X., Hamamichi, S., Ajjuri, R.R., Mazzulli, J.R., Zhang, M.W., Daigle, J.G., Zhang, S., Borom, A.R., Roberts, L.R. *et al.* (2014) The glycolytic enzyme, GPI, is a functionally conserved modifier of dopaminergic neurodegeneration in Parkinson's models. *Cell Metab.*, **20**, 145–157.
15. Murphy, C.T., McCarroll, S.A., Bargmann, C.I., Fraser, A., Kamath, R.S., Ahringer, J., Li, H. and Kenyon, C. (2003) Genes that act downstream of DAF-16 to influence the lifespan of *Caenorhabditis elegans*. *Nature*, **424**, 277–283.
16. Suzuki, R., Lee, K., Jing, E., Biddinger, S.B., McDonald, J.G., Montine, T.J., Craft, S. and Kahn, C.R. (2010) Diabetes and insulin in regulation of brain cholesterol metabolism. *Cell Metab.*, **12**, 567–579.
17. Uhlén, M., Fagerberg, L., Hallström, B.M., Lindskog, C., Oksvold, P., Mardinoglu, A., Sivertsson, Å., Kampf, C., Sjöstedt, E., Asplund, A. *et al.* (2015) Tissue-based map of the human proteome. *Science*, **347**, 1260419.
18. Levin, M., Hashimshony, T., Wagner, F. and Yanai, I. (2012) Developmental milestones punctuate gene expression in the *Caenorhabditis* embryo. *Dev. Cell*, **22**, 1101–1108.
19. Igarashi, M., Osuga, J.I., Uozaki, H., Sekiya, M., Nagashima, S., Takahashi, M., Takase, S., Takanashi, M., Li, Y., Ohta, K. *et al.* (2010) The critical role of neutral cholesterol ester hydrolase 1 in cholesterol removal from human macrophages. *Circ. Res.*, **107**, 1387–1395.
20. Okazaki, H., Igarashi, M., Nishi, M., Sekiya, M., Tajima, M., Takase, S., Takanashi, M., Ohta, K., Tamura, Y., Okazaki, S. *et al.* (2008) Identification of neutral cholesterol ester hydrolase, a key enzyme removing cholesterol from macrophages. *J. Biol. Chem.*, **283**, 33357–33364.
21. Chiang, K.P., Niessen, S., Saghatelian, A. and Cravatt, B.F. (2006) An Enzyme that Regulates Ether Lipid Signaling

Pathways in Cancer Annotated by Multidimensional Profiling. *Chem. Biol.*, **13**, 1041–1050.
22. Pani, A., Dessì, S., Diaz, G., La Colla, P., Abete, C., Mulas, C., Angius, F., Cannas, M.D., Orru, C.D., Cocco, P.L. *et al.* (2009) Altered cholesterol ester cycle in skin fibroblasts from patients with Alzheimer's disease. *J. Alzheimers. Dis.*, **18**, 829–841.
23. Rauthan, M. and Pilon, M. (2011) The mevalonate pathway in *C. elegans*. *Lipids Health Dis.*, **10**, 243.
24. Björkhem, I., Meaney, S. and Fogelman, A.M. (2004) Brain Cholesterol: Long Secret Life behind a Barrier. *Arterioscler. Thromb. Vasc. Biol.*, **24**, 806–815.
25. Stout, R.F., Verkhratsky, A. and Parpura, V. (2014) *Caenorhabditis elegans* glia modulate neuronal activity and behavior. *Front Cell Neurosci.*, **8**, 67.
26. Igarashi, M., Osuga, J.-I., Isshiki, M., Sekiya, M., Okazaki, H., Takase, S., Takanashi, M., Ohta, K., Kumagai, M., Nishi, M. *et al.* (2010) Targeting of neutral cholesterol ester hydrolase to the endoplasmic reticulum via its N-terminal sequence. *J. Lipid Res.*, **51**, 274–285.
27. Etingin, O.R. and Hajjar, D.P. (1985) Nifedipine increases cholesteryl ester hydrolytic activity in lipid-laden rabbit arterial smooth muscle cells. A possible mechanism for its antiatherogenic effect. *J. Clin. Invest.*, **75**, 1554–1558.
28. Sekiya, M., Osuga, J.I., Nagashima, S., Ohshiro, T., Igarashi, M., Okazaki, H., Takahashi, M., Tazoe, F., Wada, T., Ohta, K. *et al.* (2009) Ablation of Neutral Cholesterol Ester Hydrolase 1 Accelerates Atherosclerosis. *Cell Metab.*, **10**, 219–228.
29. Sozen, E. and Ozer, N.K. (2017) Impact of high cholesterol and endoplasmic reticulum stress on metabolic diseases: An updated mini-review. *Redox Biol.*, **12**, 456–461.
30. Hamamichi, S., Rivas, R.N., Knight, A.L., Cao, S., Caldwell, K.A. and Caldwell, G.A. (2008) Hypothesis-based RNAi screening identifies neuroprotective genes in a Parkinson's disease model. *Proc. Natl. Acad. Sci. U. S. A*, **105**, 728–733.
31. de Lau, L.M. and Breteler, M.M. (2006) Epidemiology of Parkinson's disease. *Lancet. Neurol.*, **5**, 525–535.
32. Bansal, A., Zhu, L.J., Yen, K. and Tissenbaum, H.A. (2015) Uncoupling lifespan and healthspan in *Caenorhabditis elegans* longevity mutants. *Proc. Natl. Acad. Sci.*, **112**, E277–E286.
33. Hope, I.A. (1999) *C. elegans - A Practical Approach*. Oxford University Press.
34. Zhang, J. and Liu, Q. (2015) Cholesterol metabolism and homeostasis in the brain. *Protein Cell*, **6**, 254–264.
35. Soccio, R.E. (2004) Intracellular cholesterol transport. *Arterioscler. Thromb. Vasc. Biol.*, **24**, 1150–1160.
36. Tabas, I. (2002) Consequences of cellular cholesterol accumulation: Basic concepts and physiological implications. *J. Clin. Invest.*, **110**, 905–911.
37. Graham, A., Angell, A.D.R., Jepson, C.A., Yeaman, S.J. and Hassall, D.G. (1996) Impaired mobilisation of cholesterol from stored cholesteryl esters in human (THP-1) macrophages. *Atherosclerosis*, **120**, 135–145.
38. Yancey, P.G., Bortnick, A.E., Kellner-Weibel, G., De la Llera-Moya, M., Phillips, M.C. and Rothblat, G.H. (2003) Importance of different pathways of cellular cholesterol efflux. *Arterioscler. Thromb. Vasc. Biol.*, **23**, 712–719.
39. Morel, D.W. and Lin, C.Y. (1996) Cellular biochemistry of oxysterols derived from the diet or oxidation in vivo. *J. Nutr. Biochem.*, **7**, 495–506.
40. Zhao, B., Song, J., St Clair, R.W. and Ghosh, S. (2007) Stable overexpression of human macrophage cholesteryl ester hydrolase results in enhanced free cholesterol efflux from human THP1 macrophages. *Am. J. Physiol. Cell Physiol.*, **292**, C405–C412.
41. Ascherio, A., Weisskopf, M.G., O'Reilly, E.J., McCullough, M.L., Calle, E.E., Rodriguez, C. and Thun, M.J. (2004) Coffee consumption, gender, and Parkinson's disease mortality in the Cancer Prevention Study II cohort: The modifying effects of estrogen. *Am. J. Epidemiol.*, **160**, 977–984.
42. Chang, T.-Y., Chang, C.C.Y., Ohgami, N. and Yamauchi, Y. (2006) Cholesterol sensing, trafficking, and esterification. *Annu. Rev. Cell Dev. Biol.*, **22**, 129–157.
43. Raychaudhuri, S., Im, Y.J., Hurley, J.H. and Prinz, W.A. (2006) Nonvesicular sterol movement from plasma membrane to ER requires oxysterol-binding protein-related proteins and phosphoinositides. *J. Cell Biol.*, **173**, 107–119.
44. Underwood, K.W., Jacobs, N.L., Howley, A. and Liscum, L. (1998) Evidence for a cholesterol transport pathway from lysosomes to endoplasmic reticulum that is independent of the plasma membrane. *J. Biol. Chem.*, **273**, 4266–4274.
45. Sugii, S., Reid, P.C., Ohgami, N., Du, H. and Chang, T.Y. (2003) Distinct endosomal compartments in early trafficking of low density lipoprotein-derived cholesterol. *J. Biol. Chem.*, **278**, 27180–27189.
46. Wang, L., Schuster, G.U., Hultenby, K., Zhang, Q., Andersson, S. and Gustafsson, J.-A. (2002) Liver X receptors in the central nervous system: from lipid homeostasis to neuronal degeneration. *Proc. Natl. Acad. Sci. U. S. A*, **99**, 13878–13883.
47. Fantini, J., Carlus, D. and Yahi, N. (2011) The fusogenic tilted peptide (67-78) of α-synuclein is a cholesterol binding domain. *Biochim. Biophys. Acta - Biomembr.*, **1808**, 2343–2351.
48. Aufschnaiter, A., Kohler, V., Diessl, J., Peselj, C., Carmona-Gutierrez, D., Keller, W. and Büttner, S. (2017) Mitochondrial lipids in neurodegeneration. *Cell Tissue Res.*, **367**, 125–140.
49. Snead, D. and Eliezer, D. (2014) α-Synuclein Function and Dysfunction on Cellular Membranes. *Exp. Neurobiol.*, **23**, 292–313.
50. Chiba, T., Ikeda, M., Umegaki, K. and Tomita, T. (2011) Estrogen-dependent activation of neutral cholesterol ester hydrolase underlying gender difference of atherogenesis in apoE$^{-/-}$ mice. *Atherosclerosis*, **219**, 545–551.
51. Stockhaus, J., Nagatani, A., Halfter, U., Kay, S., Furuya, M. and Chua, N.H. (1992) Serine-to-alanine substitutions at the amino-terminal region of phytochrome A result in an increase in biological activity. *Genes Dev.*, **6**, 2364–2372.
52. Ray, A., Zhang, S., Rentas, C., Caldwell, K.A. and Caldwell, G.A. (2014) RTCB-1 Mediates Neuroprotection via XBP-1 mRNA Splicing in the Unfolded Protein Response Pathway. *J. Neurosci.*, **34**, 16076–16085.
53. Cao, S., Gelwix, C.C., Caldwell, K.A. and Caldwell, G.A. (2005) Torsin-mediated protection from cellular stress in the dopaminergic neurons of *Caenorhabditis elegans*. *J. Neurosci.*, **25**, 3801–3812.
54. Brenner, S. (1974) The Genetics of *Caenorhabditis elegans*. *Methods*, **77**, 71–94.
55. Cooper, A., Gitler, A., Cashikar, A., Haynes, C., Hiil, K., Bhullar, B., Liu, K., Xu, K., Strathearn, K.E., Liu, F. *et al.* (2006) α-synuclein blocks ER-golgi traffic and Rab1 rescues neuron loss in Parkinson's models. ***Science***, **452**, 324–329.
56. Harrington, A.J., Yacoubian, T.A., Slone, S.R., Caldwell, K.A. and Caldwell, G.A. (2012) Functional analysis of VPS41-mediated neuroprotection in *Caenorhabditis elegans* and mammalian models of Parkinson's disease. *J. Neurosci*, **32**, 2142–2153.
57. Kamath, R.S. and Ahringer, J. (2003) Genome-wide RNAi screening in *Caenorhabditis elegans*. *Methods*, **30**, 313–321.

58. Fire, A., Xu, S., Montgomery, M.K., Kostas, S.A., Driver, S.E. and Mello, C.C. (1998) Potent and specific genetic interference by double-stranded RNA in *Caenorhabditis elegans*. *Nature*, **391**, 806–811.
59. Kain, V., Kapadia, B., Misra, P. and Saxena, U. (2015) Simvastatin may induce insulin resistance through a novel fatty acid mediated cholesterol independent mechanism. *Sci. Rep.*, **5**, 13823.
60. Babini, G., Morini, J., Baiocco, G., Mariotti, L. and Ottolenghi, A. (2015) In vitro γ-ray-induced inflammatory response is dominated by culturing conditions rather than radiation exposures. *Sci. Rep.*, **5**, 9343.
61. Lionaki, E. and Tavernarakis, N. (2013) Assessing aging and senescent decline in *Caenorhabditis elegans*: cohort survival analysis. *Methods Mol. Biol.*, **965**, 473–484.
62. Locke, C.J., Kautu, B.B., Berry, K.P., Lee, S.K., Caldwell, K.A. and Caldwell, G.A. (2009) Pharmacogenetic analysis reveals a post-developmental role for Rac GTPases in *Caenorhabditis elegans* GABAergic neurotransmission. *Genetics*, **183**, 1357–1372.
63. Schulz, T.J., Zarse, K., Voigt, A., Urban, N., Birringer, M. and Ristow, M. (2007) Glucose restriction extends *Caenorhabditis elegans* life span by inducing mitochondrial respiration and increasing oxidative stress. *Cell Metab.*, **6**, 280–293.
64. Chen, P., Burdette, A.J., Porter, J.C., Ricketts, J.C., Fox, S.A., Nery, F.C., Hewett, J.W., Berkowitz, L.A., Breakefield, X.O., Caldwell, K.A. *et al.* (2010) The early-onset torsion dystonia-associated protein, torsinA, is a homeostatic regulator of endoplasmic reticulum stress response. *Hum. Mol. Genet.*, **19**, 3502–3515.